Food Packaging and Shelf Life 34 (2022) 100944

Contents lists available at ScienceDirect

Food Packaging and Shelf Life

journal homepage: www.elsevier.com/locate/fpsl

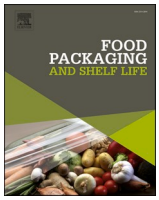

Combining experiments and mechanistic modeling to compare ventilated packaging types for strawberries from farm to retailer

Seraina Schudel [a,1], Chandrima Shrivastava [a,b,1], Séverine Gabioud Rebeaud [c], Lena Karafka [c], Kanaha Shoji [a], Daniel Onwude [a], Thijs Defraeye [a,*]

[a] Empa, Swiss Federal Laboratories for Material Science and Technology, Laboratory for Biomimetic Membranes and Textiles, Lerchenfeldstrasse 5, CH-9014 St. Gallen, Switzerland
[b] University of Bern, ARTORG Center for Biomedical Engineering Research, Murtenstrasse 50, CH-3008 Bern, Switzerland
[c] Agroscope Research Center, 1964 Conthey, Switzerland

ARTICLE INFO

Keywords:
Fruit quality
Climate chamber
Mechanistic modeling
Sensor data
Multiphysics
Food loss

ABSTRACT

Soft fruits like strawberries are highly perishable and susceptible to postharvest decay caused by fungal infestation. Mold growth is favored by elevated temperatures in the cold chain or when water vapor condenses in the packaging induced by temperature fluctuations at high relative humidity. Optimal packaging for these products is required to improve homogenous fruit cooling and ventilation inside the package along the entire supply chain. This study analyzed three packaging types (top sealed paperboard, open and closed plastic clamshell) through laboratory storage experiments and simulations. We tested the different packages in a climate chamber, with conditions representing an actual supply chain from farm to retailer. We evaluated the performance of these packages by quality measurements. We measured the fruit mass loss, total soluble solids and acidity content, firmness, color change, and incidence of decay. We also developed physics-based models for the strawberries and packaging to gain complementary information that is difficult to quantify experimentally. These models rely on mechanistic simulations and sensor data to capture fruit's hygrothermal and physiological evolution. To this end, we used monitored sensor data from the lab experiments as input for these physics-based digital fruit twins. We quantified in-silico the time of wetness due to condensation, respiration-driven overall fruit quality, and remaining shelf life along the simulated supply chain. Altogether, our simulation findings revealed that the top sealed paperboard packaging had the best performance in terms of respiration-dependent quality, mass loss and time of wetness. Furthermore, this package showed the least heterogeneities of fruit quality attributes inside the packaging, most likely due to the presence and position of ventilation holes. No clear differences were observed during laboratory experiments in rot incidence and traditional measured quality metrics (i.e., total soluble solids, acidity, color). Combining experiments with mechanistic modeling provides a deeper understanding of how fruit evolves in a supply chain. Also, it can capture packaging evaluating metrics, including moisture loss, time of wetness, or risk for microbial decay in a spatiotemporal manner.

1. Introduction

Strawberry (*Fragaria* × *ananassa*) is a popular dessert and snack fruit that is susceptible to postharvest diseases due to its high respiration rate. Gray mold rot induced by the fungal pathogen *Botrytis cinerea* is the major causal agent of immense postharvest losses of these and other soft fruits (Feliziani & Romanazzi, 2016; Williamson et al., 2007). During the winter periods in Europe, large quantities of berries are usually imported from southern European countries, often by going through a typical cold chain spanning several days (i.e., precooling, packaging, transport, distribution, retail) (do Nascimento Nunes et al., 2014; Shoji et al., 2022). Underlying drivers for the spoilage of these delicate fruits are cold chain temperature excursions out of the optimal storage range and condensation in the packaging (Bovi et al., 2019; Lai et al., 2011; Shin et al., 2007). The effect of temperature abuse or condensation is not detected along the cold chain and only appears at the retail stage in the

* Corresponding author.
E-mail address: thijs.defraeye@empa.ch (T. Defraeye).
[1] Seraina Schudel and Chandrima Shrivastava contributed equally to this paper.

https://doi.org/10.1016/j.fpsl.2022.100944
Received 29 April 2022; Received in revised form 9 September 2022; Accepted 11 September 2022
Available online 25 September 2022

form of decayed fruit. Furthermore, temperature fluctuation and improper packaging leading to inadequate ventilation and cooling can favor germination and mold growth of the ubiquitous fungal spores, usually abundant in the field, air, or through infected surrounding fruits. Therefore, the packaging design plays a crucial role in guaranteeing optimal fruit quality.

Today, a wide variety of different packaging types are available on the market (Hancock, 2020). These packages include various sizes, designs, and materials, with the trend moving more and more towards sustainable packaging solutions with reduced plastic consumption. At the same time, it is to be noted that choosing non-optimal packaging, leading to more postharvest losses, can also increase the total environmental footprint of a value chain. On the other hand, it is challenging for stakeholders to choose the right packaging type in terms of least condensation occurrences and microbial decay. The reason is that each supply chain has different cooling specifications, unit operations and duration, leading to individual hygrothermal conditions and packaging requirements. As such, each supply chain has a packaging that fits the specific needs to provide optimal quality retention and avoid spoilage.

Studies investigating optimal packaging from farm to retail, including shelf life experiments and the simulation of different cold chain segments, are scarce (Junior et al., 2019a; Kelly et al., 2019). A reason for this can be the complex nature of such experiments with real fruits. Usually, there are several limiting factors, including fruit variability, measuring decay and amount control of fungal spores, or the availability of proper climatic chambers to reproduce specific cold chains realistically. Previous studies have discussed the optimal design of (ventilated) packaging in order to make cooling processes (e.g., precooling) more efficient (Ferrua & Singh, 2011; Nalbandi & Seiiedlou, 2020). Furthermore, it was investigated how humidity-related effects impact the shelf life of packed strawberries. These studies were performed using transpiration models in order to improve modified atmosphere packaging (Sousa-Gallagher et al., 2013; Zhao et al., 2019) or humidity absorbing trays (Bovi, Caleb, Klaus, et al., 2018; Jalali et al., 2019). Nevertheless, laboratory experiments and simulation models are rarely combined when studying different fruit packaging. Besides, authors seldom addressed entire cold chains, including segments with varying conditions (temperature, humidity, air velocity). However, this is important as each unit operation induces a different type of quality loss. At retail, for example, the temperature is elevated and the humidity is low, which leads to temperature-driven quality loss. In other refrigerated unit operations, condensation and mold growth could occur due to the elevated humidity levels.

This paper presents a dual approach aiming to evaluate the packaging performance of a ventilated clamshell (open & closed) and a top sealed paperboard tray for strawberry fruits. To this end, we combine laboratory experiments with physics-based simulation in order to evaluate complementary metrics of fruit quality and marketability. We link the experiment and simulations with sensor data for hygrothermal environmental conditions representing an actual supply chain from farm to retailer, so spanning a large part of the postharvest supply chain. We analyze the impact of a commercial import supply chain, having segments with different hygrothermal conditions, on condensation occurrences and fruit quality. Classical quality parameters (i.e., total soluble solids (TSS), acidity, mass loss, firmness, color) and the amount of decay of naturally infected strawberries (cv. 'Murano') are assessed with storage and shelf life experiments. By physics-based digital twin models built for strawberries and tested packages, additional parameters are determined (i.e., volume-averaged fruit temperature, respiration-driven fruit quality, mass loss, and residence time of the condensate). Thereby, we gain complementary insights regarding the spatial heterogeneity within a package and critical areas with a high risk of condensation, among others. This information is unique and otherwise difficult to assess experimentally. Furthermore, we propose a concept for future packaging analyses that include experiments in climacteric chambers with enhanced control of hygrothermal conditions using real monitoring sensor data. Combined with simulation experiments, this will improve future packaging evaluations to identify and design an optimal package type from farm to fork.

2. Materials and methods

2.1. Laboratory quality and shelf life experiments

2.1.1. Fruit and packaging samples

Strawberries (*fragaria x ananassa*, cv. 'Murano') grown in soilless culture under a tunnel in 2021 at Agroscope Research Center (Valais, Switzerland) were used for this study. The experiment was repeated three times, and for this, strawberries were harvested weekly (test 1: 06.23.2021, test 2: 06.30.2021, and test 3: 07.07.2021) and randomly separated in triplicates in three different types of packages with a capacity of 500 g, as illustrated in Fig. 1.

2.1.2. Reproduced supply chain from farm to retail store

After harvest and packing, a strawberry import cold chain was reproduced hygrothermally in the laboratory (Fig. 2). The berries were stored at at 1 °C and 95% relative humidity (RH) for 5 days (Fig. 2(i) - 2 (iii)). This time frame is representative of a postharvest supply chain from the packing house (supplier), through the refrigerated transport, to the distribution center. Strawberries were then stored at 6 °C and 13 °Ceach for 4 h at 85% RH, to resemble a temperature ramp-up (e.g., during transport and storage to/at retail with mixed loads) (Fig. 2(iv)). Finally, berries were kept at shelf life conditions (20 °C, 90% RH) for two days, representing possible conditions at retail and the consumer's place (Fig. 2(v)). These hygrothermal conditions were indicative of measurements that we performed in an actual supply chain from farm to retailer. Temperature and relative humidity were monitored inside the package headspace throughout the reproduced supply chain using SHT31 type sensors for all triplicates (Sensirion AG, Switzerland). For test 3 and packaging type C, hygrothermal data of only two instead of three replicates could be received. One NTP-probe sensor (Ecolog TN2 type, Elpro AG, Switzerland) was inserted inside one strawberry of each package type for flesh temperature monitoring.

2.1.3. Fruit quality metrics

Quality analyses were performed on samples of 60 berries per package type (3 ×20 berries) at harvest and after storage of seven days. Fruit color was measured using a CM-600d spectrophotometer (Konica Minolta, Japan) in CIE L*a*b* color space and was expressed in terms of lightness 'L* ', 'a* ' and hue angle 'h°' (arctan (b*/a*). Texture measurements were performed with a texturometer (TA-XTplus Texture Analyzer, Stable Micro Systems, UK) fitted with a stainless puncture probe of 2 mm diameter. The probe was moved at a speed of 5 mm/sec to a final depth of 7 mm. For each measurement, a force/displacement curve was obtained, and parameters were extracted. Firmness was defined as the maximal force applied to move the probe into the flesh until 7 mm.

Juice of 3 batches of 20 berries per package type was then extracted to measure total soluble solids (TSS, %Brix) with an electronic refractometer (PAL-1, Atago, Japan) and acidity (meq/100 g) by titration (Titrator DL67, Mettler-Toledo GmbH, Switzerland) with 0.1 M NaOH to the endpoint of 8.1.

Mass loss after storage was determined by measuring fruit weight in each package at harvest and after storage. After storage, fruit decay and

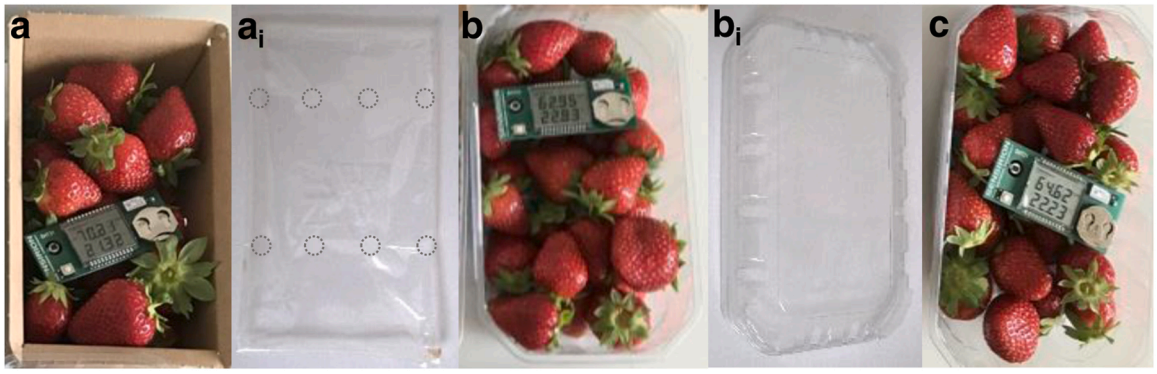

Fig. 1. Tested packaging (a) paperboard tray closed by (a_i) top sealed plastic foil with ventilation holes (dashed), (b) plastic clamshell closed by (b_i) ventilated plastic lid, and (c) open plastic clamshell without lid.

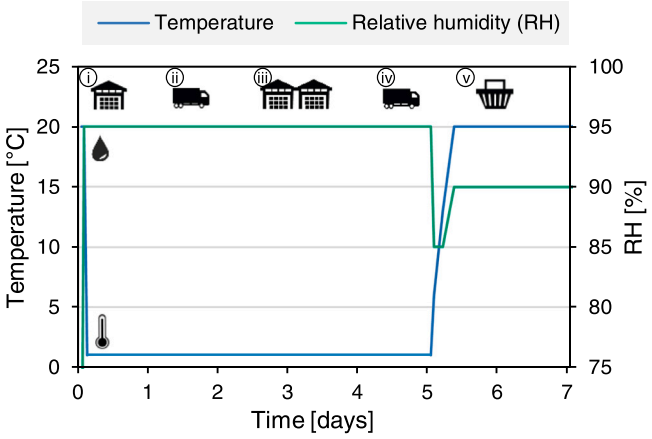

Fig. 2. Reproduced supply chain of imported strawberries, showing the temperature and relative humidity profiles that were maintained in the laboratory experiments. The segments represent different unit operations in the strawberry supply chain: (i) packing and precooling, (ii) refrigerated transport and distribution, (iii) temperature ramp-up at the retailer, (iv) redistribution to the retail store, and (v) ambient conditions during product display and at the consumer stage.

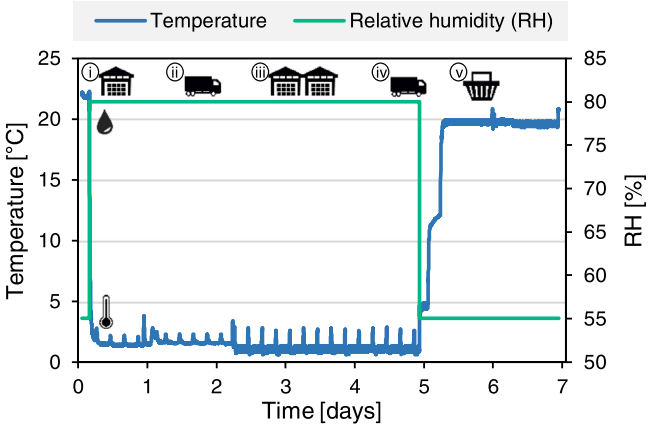

Fig. 3. Simulated supply chain of imported strawberries that was used in the physics-based model. Here, the segments correspond to different unit operations: (i) packing and precooling, (ii) refrigerated transport and distribution, (iii) temperature ramp-up at the retailer, (iv) redistribution to the retail store, and (v) ambient conditions during product display and at the consumer stage. This hygrothermal profile was used as input for the simulated packages.

percentage of shiny fruits were assessed on 60 strawberries per package type (3 ×20 fruits). Decay was expressed as an index using a 4-level severity scale based on the percentage of fruit surface affected by decay; 0: no decay, 1: < 10%, 2: 10–50%, and 3: > 50% of decay. The decay index was calculated as follows:

$$Decay\ \ severity\ \ index = \sum \frac{number\ \ of\ \ affected\ \ fruit\ \ x\ \ severity\ \ level}{total\ \ number\ \ of\ \ fruit\ \ x\ \ maximal\ \ severity\ \ level} x\ \ 100 \quad (1)$$

2.2. Physics-based digital twins of strawberries and packaging

2.2.1. Simulated supply chain from farm to retail store

The simulated hygrothermal profile corresponded to the strawberry postharvest supply chain from the farm to the retail store (Fig. 3). The different segments corresponded to the various unit operations in the strawberry supply chain (Fig. 3(i) – 3(v)). The air temperature data was based on one of the measured temperature profiles from the experimental setup (test 3, Section 2.1.2). The relative humidity was assumed to correspond to the respective unit operation, as the measured values from the storage experiments did not meet the typical range encountered in a cold chain. In the cold chain operations, the relative humidity of the surrounding air was set to 80%, and under ambient conditions, the relative humidity of the air was assumed to be 55%. Note that the relative humidity inside the fruit packaging headspace is typically much higher and close to saturation levels. The air speed was also assumed to represent indicative ranges for the unit operation (Section 2.2.2). Also note that for the physics-based model, fluctuations were also considered in the input temperature profile (Fig. 3). This was not the case for the laboratory experiments, as the fruit were stored at constant temperatures (Fig. 2).

2.2.2. Computational system configuration

An extensive three-dimensional mechanistic model was developed to simulate horizontal airflow across a single package of strawberries in a

Package type	Image of the package	Packaging material(s)	Package dimensions (length x width x height, cm)	Number of fruits in the package	Top view of the package	Side view (in flow direction) of the package
A Tray top sealed by foil	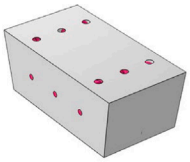	Paperboard tray, low density polyethylene foil	17 x 9 x 6.5	24	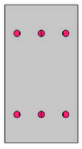	
B Clamshell closed by lid	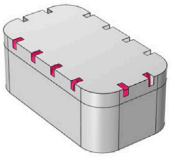	Polyethylene terephthalate tray and lid	17 x 9 x 6.5	24	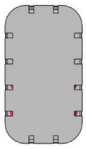	
C Unlidded (open) clamshell	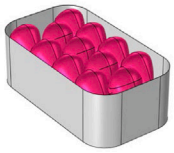	Polyethylene terephthalate tray	17 x 9 x 6.5	24		

Fig. 4. Description of the three simulated packages, including packaging materials, dimensions, number of fruits, and images of the top and side views.

channel without bypass. The model description, calibration, and validation are elaborated in (Shrivastava et al., 2022) and described in brief. Each package configuration was filled with equi-sized strawberries (equatorial diameter = 30 mm, mass = 16.2 g, surface area = 33.06 $\times 10^{-4}$ m^2). Three different packages were simulated, each containing 24 berries in a regular arrangement and a net weight of 388 g, intended for a 350 g package. Details of the three packaging are summarized in Fig. 4.

2.2.3. Flow field

A uniform upstream speed (U_{inlet}, m•s^{-1}) was defined based on indicative ranges for the superficial air speeds in the respective unit operations. This value is set to 0.01 m•s^{-1} for retail and refrigerated storage, 0.1 m•s^{-1} for refrigerated transport, and 1.0 m•s^{-1} for precooling (Han et al., 2017; Li et al., 2021; Opara & Zou, 2007; Thompson et al., 2008; Wu et al., 2019). The continuity and Navier Stokes equations were used to estimate the flow field in the air domain. To account for the turbulence effects, we use a k-ε turbulence model with wall functions. The flow field was computed in advance and then used as input for the heat and moisture transport equations.

2.2.4. Heat transport

Heat transfer in the air domain was computed using Eq. 2.

$$\rho_a c_{p,a} \frac{\partial T_a}{\partial t} + \rho_a c_{p,a}(\mathbf{u}\cdot\nabla T_a) = \nabla\cdot(k_a \nabla T_a) \quad (2)$$

where **u** is the velocity field vector, ρ_a is the density of air (1.247 kg•m^{-3}), T_a is the air temperature (K), $c_{p,a}$ is the specific heat capacity of air (1006 J•$kg^{-1}K^{-1}$), and k_a is the thermal conductivity of air (0.024 W•m^{-1}•K^{-1}) (ASHRAE, 2010). The walls of the package were modeled as 'thin layers' offering a certain thermal resistance. Heat transfer in the fruit domain is described in Eq. 3.

$$\rho_f c_{p,f} \frac{\partial T_f}{\partial t} = \nabla\cdot(k_f \nabla T_f) + Q_{resp} \quad (3)$$

where T_f is the fruit temperature (in K) at any time instant t, k_f is the thermal conductivity of strawberry (0.6 W•m^{-1}•K^{-1}), $c_{p,f}$ is the specific heat capacity of strawberry (4000 J•kg^{-1}•K^{-1}), ρ_f is the density of the strawberry (961 kg•m^{-3}), and Q_{resp} is the volumetric heat of respiration as a function of temperature (W•m^{-3}). The heat of respiration was 40 mW•kg^{-1} at 0 °C, 150 mW•kg^{-1} at 10 °C, and 400 mW•kg^{-1} at 20 °C (Becker et al., 1996).

The initial temperature of the system was assumed 20 °C. In this study, we assumed that the strawberry package is in the vicinity of the air temperature sensor. The air temperature upstream of the package at the inlet ($T_{upstream}$, K) is defined as a function of time-based on measured data.

2.2.5. Moisture transport

The moisture transport in the computational domain, namely air, is described using Eq. 4.

$$M_v \mathbf{u}\cdot\nabla c_v + \nabla\cdot(-M_v D_{v,a} \nabla c_v) = G \quad (4)$$

Here M_v is the molar mass of water vapor (18 $\times 10^{-3}$ kg•mol^{-1}), **u** is the velocity field vector (m•s^{-1}), c_v is the vapor concentration (mol•m^{-3}), and $D_{v,a}$ is the water vapor diffusion coefficient of air (2.4 $\times 10^{-5}$ m^2•s^{-1}). The source term (G, kg•m^{-3}•s^{-1}) represents the addition or removal of moisture within the domain, due to evaporation or condensation, which is non-zero at the fruit surface. Water vapor transport across the package walls is modeled using the thickness of the packaging material (x_p, m) and the water vapor resistance factor (μ_p, -). The water vapor resistance factor is the ratio of water vapor permeability of air to the water vapor permeability of the packaging material. This value was in the range of 0.7 × 10^6 – 8.5 × 10^6 for the packaging materials, which is rather high as these packaging materials are vapor tight.

Moisture loss (water vapor) flux at the fruit surface ($g_{v,evap}$, kg•m^2•s^{-1}) is computed using Eq. 5.

$$\mathbf{n}\cdot\mathbf{g}_{v,evap} = k_{skin} M_v (a_w \cdot c_{sat} - c_v) \text{if}(a_w \cdot c_{sat} > c_v) \quad (5)$$

where k_{skin} is the skin resistance to moisture transport (1.77 $\times 10^{-3}$ m•s^{-1}), c_{sat} is the saturation concentration of vapor (mol•m^{-3}), and a_w is the water activity at the fruit surface (0.997) (Becker et al., 1996). The net mass loss in the fruit is accounted for as the combined contribution of moisture loss due to transpiration and dry weight loss during respiration by integrating the evaporation flux ($g_{v,evap}$).

Condensation was assumed to take place when the surface temperature of the fruit or tray was below the dew point temperature of the air.

The liquid water concentration on the surface at any given point of time (c_l, mol•m^{-2}) was computed using Eq. 6.

$$M_v \frac{\partial c_l}{\partial t} = -g_{l,evap} \quad (6)$$

Here M_v is the molar mass of water vapor (18×10^{-3} kg•mol^{-1}). The liquid water flux at the fruit surface ($g_{l,evap}$, kg•m^2•s^{-1}) accounted for the condensation of liquid water, as well as the re-evaporation of this condensed water. The time of wetness (*ToW*, h) was computed as the integral of the time when the liquid water concentration on the fruit surface (c_l) is non-zero or when the relative humidity at the surface of the berry is higher than 95%, as this is critical for the growth of *Botrytis cinerea* (Jarvis, 1977; Lahlali et al., 2007; Linke & Geyer, 2013; Snow, 1949; Williamson et al., 1995).

2.2.6. Kinetic model for respiration-driven fruit quality

We modeled the respiration-driven biochemical fruit quality using a first-order kinetic model (Eq. 6).

$$-\frac{dI_f(t)}{dt} = k_{\text{quality}}(T_f) \cdot I_f(t) \quad (7)$$

where I(t) is the remaining fruit quality index (%) at any time instant t, $k_{\text{quality}}(T_f)$ is the temperature-dependent rate constant (s^{-1}), and T_f represents the temperature at any point in the fruit (K). The initial value of the fruit quality index is assumed to be 100%. In our calibration, we assumed that strawberries could be stored for about 14 days at 0 °C, for 5 days at 10 °C, and for about 2 days at 20 °C. This implies a Q_{10} value of 2.75 (Hikawa-Endo, 2020; Tano et al., 2009). In our calibration, we arbitrarily set the threshold for loss in fruit quality, and therefore end of shelf life, at a quality index of 20%. This choice of threshold ($I_f = 20\%$) does not affect the predicted shelf life at a certain temperature (Tijskens & Polderdijk, 1996). The temperature dependence of the rate constant $k_{\text{quality}}(T_f)$ is accounted for by the Arrhenius equation for reaction rates (van Boekel, 2008). Based on our calibration, the estimated pre-exponential rate constant ($k_{0,\text{quality}}$) was 3.55×10^6 s^{-1} and the estimated activation energy was 65 kJ•mol^{-1}.

2.2.7. Metrics for fruit quality evaluated for every package

The physics-based model provides the following quantified actionable metrics for strawberry in every package:

- average fruit temperature (°C);
- respiration-driven remaining fruit quality index (I_f, %);
- total mass loss (*ML*, %);
- time of wetness due to condensation (*ToW*, h).

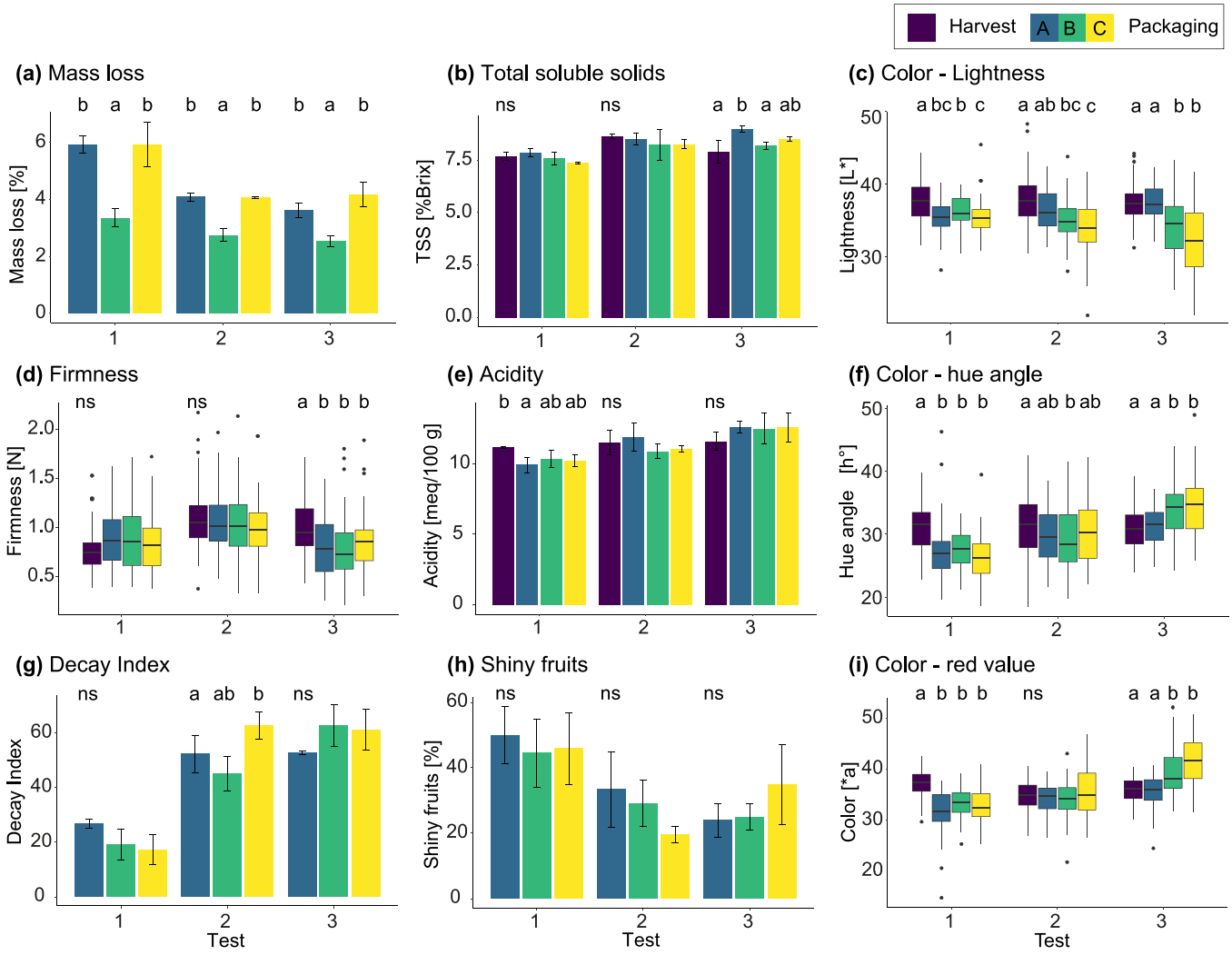

Fig. 5. Influence of packaging on (a) percentage of mass loss, (b) total soluble solids, (c) lightness (color), (d) firmness, (e) acidity, (f) hue angle (color), (g) decay index, (h) percentage of shiny fruits, and (i) red value (color) measured at harvest and after shelf life for packaging A (top sealed paperboard), B (closed clamshell), and C (open clamshell). Significant differences between packaging types of individual tests are indicated by different letters at $p \leq 0.05$ according to Tukey's (a, b, e, g, h) and Dunn's (c, d, f, i) test; ns: not significant.

2.2.8. Numerical implementation

We implemented the multiphysics model in the finite-element-based modeling software COMSOL Multiphysics (version 6.0). For the airflow, heat, and moisture transport models, we used the 'Turbulent Flow, k-ε', 'Heat Transfer in Moist Air', and 'Moisture Transport in Air' interfaces with 'Multiphysics' coupling. The kinetic model for temperature-dependent fruit quality was implemented using the 'Ordinary Differential Equation' interface. The fruit and air domains were meshed with tetrahedral elements based on a grid sensitivity analysis. A time step of 10 min was considered for the output results of the simulations.

2.3. Statistical analysis

All statistical analyses and data visualization were performed in MS Office, R version 3.6.3, COMSOL Multiphysics® (version 6.0), and Origin® 2022 (OriginLab, 2022; R Core Team, 2020). End values are reported as mean ± standard deviation. For all statistical analyses, a significance level of 5% was considered ($p \leq 0.05$). Statistically significant differences to compare the means of measured TSS, acidity, mass loss, percentage of shiny fruits, and decay index between packaging were tested using one-way analysis of variance (ANOVA) followed by Tukey's post hoc test. To compare the means of the measured values for color, firmness, and monitored temperature and humidity of different packages, we performed the Kruskal Wallis test followed by Dunn's post hoc test. The p-values were adjusted by the Benjamini-Hochberg method. One-way ANOVA followed by Tukey's test to compare means was also employed for comparing the volume-averaged fruit temperature, remaining quality index, net mass loss, and time of wetness averaged across the supply chain predicted by the simulations.

3. Results

3.1. Comparing the performance of ventilated packaging by storage experiments

3.1.1. Quality metrics at harvest and after storage at reproduced supply chain

After storage, the average mass loss of differently packed berries varied from 2.5% to 5.9% (Fig. 5, a). The measured mass loss was similar for the top sealed paperboard packaging (A) and open clamshell (C), whereas it was significantly lower for the closed clamshell (B). It is interesting to note that mass loss was higher in test 1 for all tested packages compared to tests 2 and 3. This indicates an influence of harvest date on this parameter.

In tests 1 and 2, total soluble solids (TSS) were relatively stable during storage and shelf life as these values were similar to those measured at harvest (Fig. 5, b). In test 3, berries stored in packaging A showed, on average, the highest TSS values (9% Brix) in comparison to harvest and other packages. No significant differences were measured in fruit acidity between at harvest and the end of shelf life and between the different packaging (Fig. 5, e). Similarly, the tested packages types did not influence the fruit firmness (Fig. 5, d). Firmness at harvest in tests 2 and 3 was slightly higher compared to test 1, which indicates an influence of harvest date on this parameter.

Color values were assessed as lightness (L*), red color (+a*), and hue angle (h°). Regarding the parameter L* , storage led to darker berries in comparison to harvest (Fig. 5, c). In tests 2 and 3, berries packed in the open clamshell showed the lowest L* values compared with test 1. It can be seen that measured a* and h° showed similar trends within the same tests (Fig. 5, f,i). Observed color metrics in tests 1 and 2 were in the same range for all packaging, whereas in test 3, closed and open clamshell led to higher a* and h° values than the top sealed paperboard package. Overall, the top sealed paperboard package had the lowest influence on color parameters that were closest to those measured at harvest.

The fruit decay index was similar for all tested packaging (Fig. 5, g). There was a remarkable increase in the amount of decay in tests 2 and 3 compared to test 1. The percentage of shiny fruits also did not significantly differ between the tested packaging, independently of the test. However, slightly more shiny fruits were observed in test one compared to tests two and three.

Overall, we observed the least mass loss for top sealed paperboard packaging. However, there was no package type showing the best performance regarding the quantified decay. The measured quality and shelf life attributes varied more between tests than between different packaging. This shows the difficulty of identifying statistical differences between packaging in laboratory experiments. The impact of the harvest date was considerable, especially for mass loss, decay index, and shininess.

3.1.2. Hygrothermal conditions in the packaging headspace and monitored fruit core temperature

Temperature and relative humidity were monitored during storage and reproduced supply chain, as shown for test 3 in Fig. 6. The different cold chain segments, including precooling and storage at 1 °C and

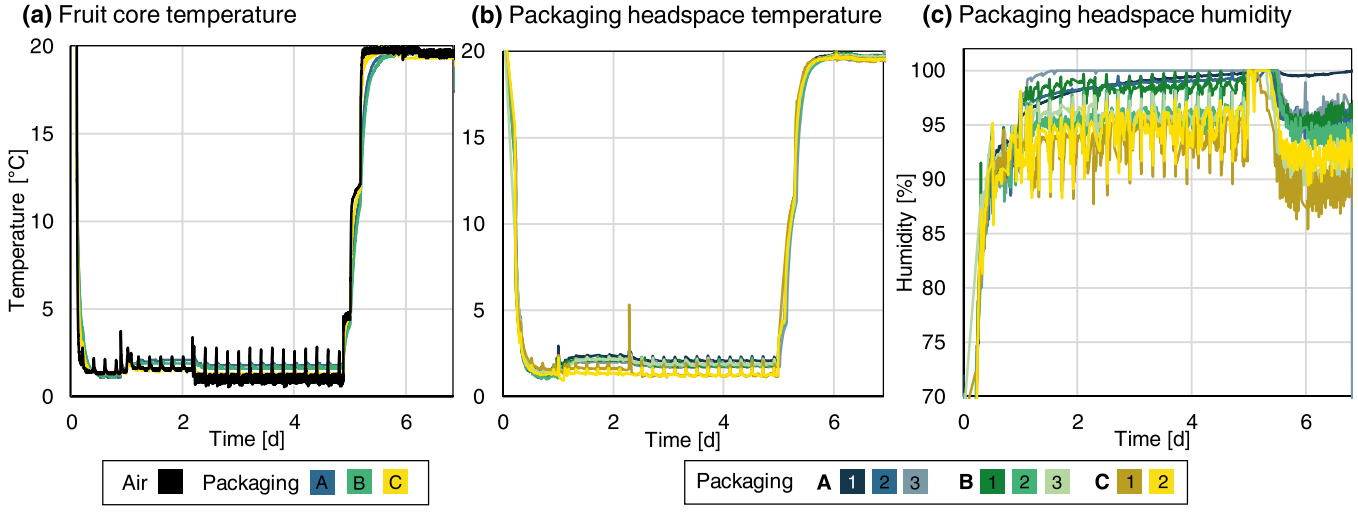

Fig. 6. Monitored sensor data for (a) air and fruit flesh temperature; (b) packaging headspace temperature (n = 8); (c) packaging headspace humidity for packaging A (top sealed paperboard), B (closed clamshell), and C (open clamshell). Fruit core temperatures were measured for one berry per packaging type, and headspace conditions were displayed for replicates of three (packaging A, B) or two (packaging C). The sensor data shown was assessed during test 3.

Table 1
Temperature and humidity monitored inside the headspace packaging after temperature conditioning and storage at 1 °C (3 days) and 20 °C (1 day) measured during test 3 using Sensirion type SHT31 sensors.

			Packaging headspace conditions							
			A1	A2	A3	B1	B2	B3	C1	C2
1 °C	Temperature	AVE±SD [°C]	2.1 ± 0.2^{a}	1.9 ± 0.2^{b}	1.8 ± 0.2^{c}	1.8 ± 0.3^{b}	1.9 ± 0.3^{d}	2.0 ± 0.3^{e}	1.4 ± 0.3^{f}	1.3 ± 0.1^{g}
	Humidity	AVE±SD [%RH]	98.7 ± 1.0^{a}	98.6 ± 0.7^{a}	99.9 ± 0.5^{b}	98.4 ± 0.6^{c}	95.5 ± 1.2^{d}	95.9 ± 0.9^{e}	93.3 ± 1.6^{f}	94.4 ± 1.7^{g}
20 °C	Temperature	AVE±SD [°C]	20.1 ± 0.9^{ab}	19.6 ± 0.5^{cd}	19.6 ± 0.5^{c}	19.8 ± 0.1^{b}	19.7 ± 0.1^{ae}	19.9 ± 0.6^{e}	19.6 ± 0.4^{cd}	19.7 ± 0.5^{d}
	Humidity	AVE±SD [%RH]	99.7 ± 0.2^{a}	95.4 ± 0.7^{b}	96.0 ± 1.0^{b}	95.7 ± 0.7^{b}	94.0 ± 0.7^{c}	90.9 ± 1.6^{d}	89.3 ± 1.1^{e}	92.0 ± 1.0^{d}

Packaging A = top sealed paperboard (n = 3); B = closed clamshell (n = 3); C = open clamshell (n = 2). Significant difference between measured temperature and humdity of tested packaging are indicated by different supscripted letters at $p \leq 0.05$.

Table 2
Monitored air and fruit temperature assessed for one fruit per packaging after temperature conditioning and storage at 1 °C (3 days) and 20 °C (1 day) measured during test 3 using Elpro type Ecolog TN2 sensors.

		Air temperature	Fruit core temperature		
			A	B	C
1 °C	AVE±SD [°C]	1.3 ± 0.5	1.9 ± 0.2^{a}	1.8 ± 0.2^{b}	1.4 ± 0.2^{c}
20 °C	AVE±SD [°C]	19.6 ± 0.2	19.5 ± 0.2^{a}	19.6 ± 0.1^{b}	19.3 ± 0.1^{c}

Packaging A = top sealed paperboard (n = 3); B = closed clamshell (n = 3); C = open clamshell (n = 2). Significant temperature variation between tested packages are indicated by different supscripted letters at $p \leq 0.05$.

temperature ramp-up (4 h at 6 °C plus 4 h at 13 °C) and storage at 20 °C can be observed (Fig. 6, a,b).

The measured temperature of the fruit and inside the different packaging was in a similar range. Nevertheless, significant differences between single packages were observed during each segment (1 °C, 20 °C) (Table 1, Table 2). For both fruit core and packaging temperature, the open clamshell packaging (C) showed the lowest temperature values that were closest to the air temperature. Temperature for the top sealed paperboard package (A) showed, on average, the highest values, but in a comparable range as the closed clamshell (B). However, the measured differences also varied for the same package type, which could indicate that the position of the packaging in the storage room has an impact on the monitored temperature. Different positions of each packaging was however not monitored. The standard deviation of the measured temperature, indicating the temperature fluctuations, showed slight variations but was in a similar range between and within different packaging types.

It can be seen that the average relative humidity throughout the storage was maintained high (90–95%) (Fig. 6, c). It should be noted that during the temperature ramp-up in the cool room, the desired humidity (≤85%) could not be reached due to the prevalent moist weather and lack of an accelerated dehumidification system. This issue led to a sudden humidity increase in almost all packaging and, most likely, condensation (Fig. 6, c). For package A, the measured humidity during storage was often close to 100%, indicating inadequate packaging

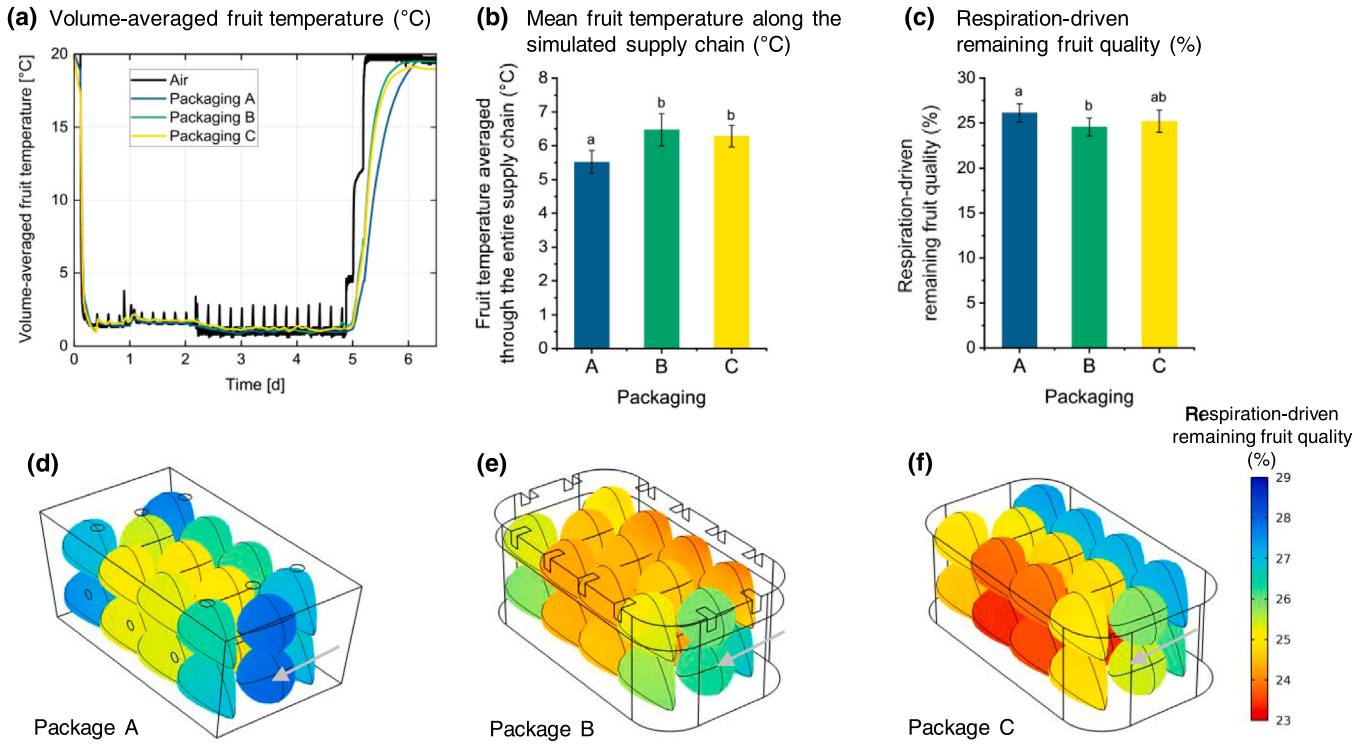

Fig. 7. Influence of packaging on temperature and respiration-driven fruit quality: (a) Temperature curves for air temperature and the volume-averaged fruit temperature in the three packaging types; (b) Mean volume-averaged fruit temperature along the entire supply chain (°C); (c) Remaining respiration-based fruit quality (%) averaged across the entire supply chain; (d, e, f) Spatial variation in respiration-driven remaining fruit quality in the tested packaging. The error bars denote the spread within the package. Significant differences between mean values of the different packaging are indicated by different superscripted letters at $p \leq 0.05$. A: top sealed paperboard tray; B: closed clamshell; C: open clamshell. The arrow indicates the flow direction.

ventilation and accumulation of condensate. As expected, package C showed the lowest humidity values. Nevertheless, storage in open trays at ambient conditions with low relative humidity leads to an increased risk of mass loss and softening symptoms.

In conclusion, the humidity variation between packaging types was more prominent than the temperature variation. Lower humidity observed for packaging C was also in line with increased mass loss in those berries compared to packaging A and B (Fig. 5). Similar temperature values can also be why quality parameters, that underline temperature-dependent kinetic reactions (e.g., TSS, color, acidity), were insignificant between the packaging types.

3.2. Comparing the performance of ventilated packaging by simulations

3.2.1. Fruit temperature and respiration-driven fruit quality

As strawberries are small fruits, they have a small Biot number (<1) along the supply chain. As a result, the fruit temperature is rather uniform throughout the fruit. The pulp temperature at any location of the fruit is representative for the average fruit temperature. We measured that differences in the mean fruit temperature in tested packages were rather small (<0.5 °C), as observed in Fig. 7, b. Thus, the respiration-driven fruit quality and remaining shelf life did not show a large difference among packages (Fig. 7, c). This also explains why we did not observe significant differences in metrics such as color, firmness, and soluble solids in the experimental study (Fig. 5). The kinetics of those metrics is governed primarily by fruit temperature.

Amongst the three packaging analyzed, the open clamshell (C) shows the largest heterogeneity in fruit temperature and thus remaining quality (Fig. 7, f). On the other hand, the closed clamshell (B) and the top sealed paperboard tray (A) showed a more uniform temperature distribution and remaining fruit quality (Fig. 7, d,e). This could be due to the presence of vents. Several studies have reported that the presence of vents, especially in the flow direction, improves cooling efficiency and uniformity (Getahun et al., 2017; Pathare et al., 2012).

3.2.2. Net transpiration-driven mass loss

The average mass loss at the end of the simulated supply chain was found to be the lowest for the top sealed paperboard tray (4.83%). On the other hand, the open clamshell (C), as well as the closed clamshell (B), showed a higher mass loss (Fig. 8, a). For open packaging C, the increased mass loss could be attributed to the top layer of fruit being exposed to the delivery air, resulting in higher moisture loss (Fig. 8, c). The package B had a higher mass loss due to the presence of vents on the lid, which allows air inside the package is replaced frequently. As a result, the net relative humidity in the package headspace was lower, increasing the driving force for transpiration. The top sealed paperboard tray showed the highest uniformity in mass loss, primarily as this packaging has vents in the flow direction.

In general, the net mass loss values were higher than those predicted experimentally. This is primarily due to two reasons. Firstly, the air speed varied depending on the unit operation in the simulation. On the other hand, the air speed was constant and relatively low in the experiments, as we could not control this in the climatic chamber. Higher air flow rates increase remove more moisture and, therefore, lead to higher net mass loss. Secondly, the relative humidity of the delivery air was set to 55% during the simulated retail unit operation. This was not achieved in the experimental study due to the limitations of the climate chamber dehumidification system.

3.2.3. Condensation and microbiological risk

The use of physics-based models allows the quantification of the risk of condensation, which takes place when the fruit surface temperature falls below the dew point temperature. The cumulative amount of condensation at the end of the supply chain did not significantly differ (Fig. 9, a). However, in Fig. 9 (b-d) the spatial variation of the simulated packaging in the risk of condensation and, consequently, mold growth inside a package can be observed. Here, we it can be seen that the fruit in the bottom layer is the most susceptible to condensation. One of the reasons could be that the packages analyzed in this study did not have vents at the bottom surface. However, this is often the case in reality, as vents on the bottom surface are partially or even completely blocked. This could be either by the fruit itself placed on top of the vent, by bubble wrap padding below the berries to minimize mechanical damage, or due to stacking of packages in a pallet.

Although the spatial region for the risk of condensation is large for the top sealed paperboard tray, the overall time of wetness averaged over the fruit surface is lower in comparison to other packages. This can be seen if we observe the risk of condensation at the bottom of the packaging. This could be due to the vents in the flow direction that constantly exchange the air inside the package, thus lowering the headspace humidity. The ventilated clamshell showed the highest risk of condensation. As condensation is a main trigger for germination of *B. cinerea* spores, these regions in the packaging also correspond to the highest microbiological risk. In summary, locations with excessive condensation inside the package should be avoided to minimize this risk that leads to prevention of the purchase by the consumer, and eventually, to spoilage. Note that here, we did not include the influence of condensation on the mechanical strength of the packaging.

4. Discussion

4.1. Shelf life experiments did not reveal a best-performing packaging

Based on the laboratory experiments, we found that closed

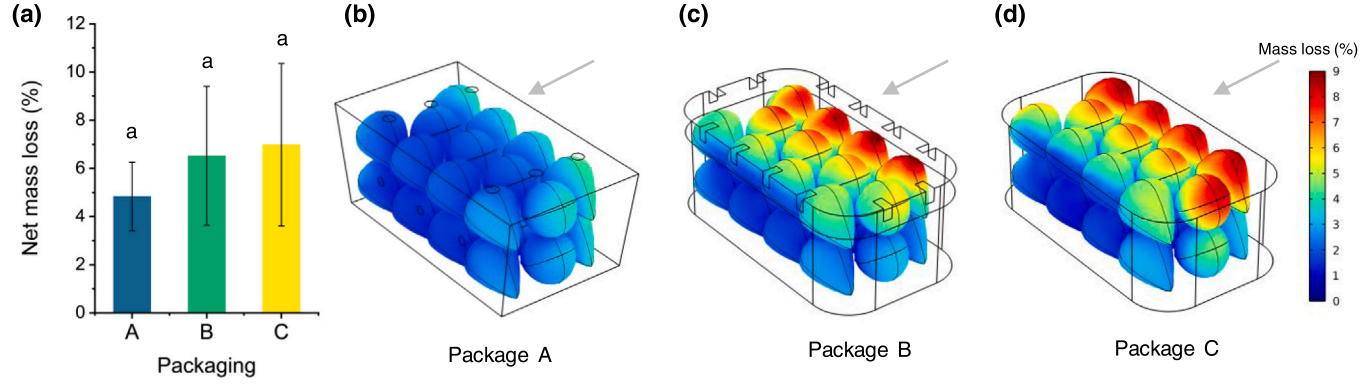

Fig. 8. Influence of packaging on (a) net mass loss (%) and (b,c,d) spatial variation in mass loss (%) at the end of the simulated supply chain for package A, B and C. The error bars denote the spread within the package. Significant differences between mean values of the different packaging are indicated by different superscripted letters at $p \leq 0.05$. A: top sealed paperboard tray; B: closed clamshell; C; open clamshell. The arrow indicates the flow direction.

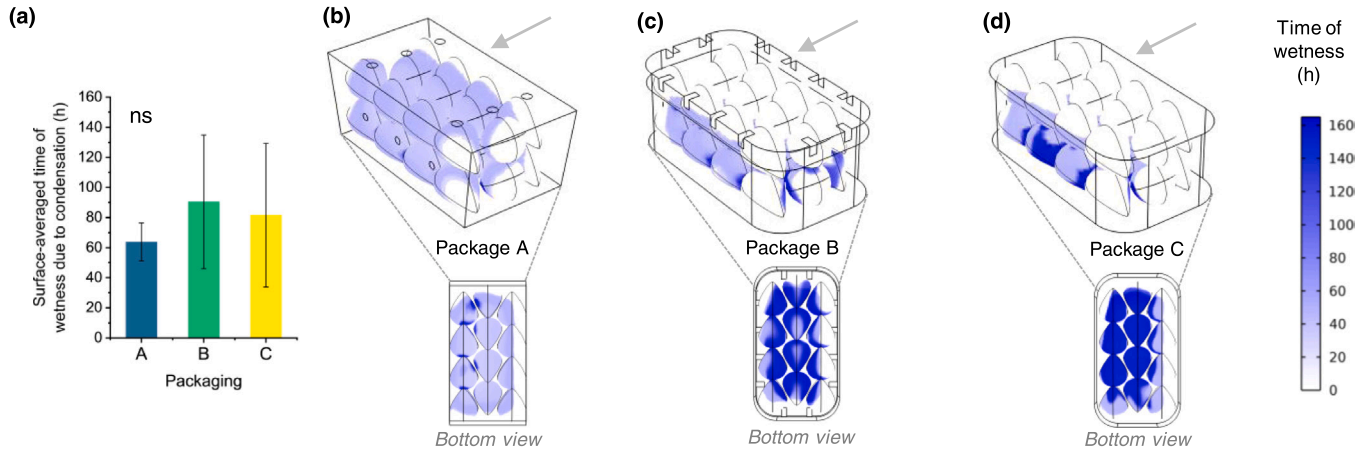

Fig. 9. Influence of packaging on the (a) risk of condensation as fruit surface-averaged time of wetness (hours); (b, c, d) spatial variation in the risk of condensation at the end of the simulated supply chain for packages A, B, and C. The error bars denote the spread within the package. Significant differences between mean values of the different packaging are indicated by different letters at $p \leq 0.05$, ns: not significant. A: top sealed paperboard tray; B: closed clamshell; C: open clamshell. The arrow indicates the flow direction.

clamshells led to the least mass loss of stored fruits, which is directly related to the salable fruit weight. A reason for the higher amount of mass loss in the closed paperboard package compared to the closed clamshell could be that the paper material can take up moisture from the berries. On the other hand, this can reduce the amount of excessive water or condensates in the packaging. Regarding microbial decay, we did not find a trend between tested packages. Based on the results, we assume that the harvest dates (e.g., variation in weather conditions, pathogen pressure, etc.) influenced the decay severity more than the different packaging types. Furthermore, the quantified traditional quality parameters did not clearly vary with package type. Similar findings were previously made, where TSS and acidity (Bovi, Caleb, Ilte, et al., 2018; Peano et al., 2014) or firmness (Al-Asmar et al., 2020) after storage did not significantly vary between tested packaging. A possible explanation could be that the measured hygrothermal conditions for fruits and packaging headspace, which influence temperature-dependent ripening reactions, were in the same range for different packages. Additionally, we assume that the storage position in the cool room, with varying cooling air velocity, could have an impact on those conditions. Identifying statistical differences between packaging in experiments is thus challenging.

Overall, a high amount of decay was monitored for all packed and stored berries (decay index >20–60). A reason for this could be the increased occurrence of extreme weather events in the season 2021 in the harvest region. Heavy rainfalls can lead to a quality decrease of harvested fruits and consequently to reduced storage or shelf life. Besides, we conclude that evaluating naturally infected fruits is challenging when comparing results from different tests, as the initial amount of fungal spores can significantly vary between fruits or tests. This was shown in previous work on grapes, where artificial infection of *B. cinerea* compared to natural infection gave more conclusive results for identifying a mold-reducing packaging type (Junior et al., 2019b).

Another limitation of this study was that not all specifications of a realistic cold chain from farm to retailer could be met by using the cold rooms, as humidity or temperature fluctuations could not entirely be controlled. This also prevented producing all condensation occurrences in the tested packaging.

4.2. Simulations provided complementary insights into the package

For the three simulated packages, we used the same fruit arrangement as well as the input air temperature profile. In this way, we could isolate small differences introduced due to the packaging. Our findings revealed that the top sealed paperboard tray (A) has the least risk of condensation. This finding is promising, given that consumers and retailers are increasingly steering away from plastic and transitioning towards sustainable packaging solutions. The package design might even be improved if vent holes were added in the top sealed paperboard trays on the bottom of the paperboard. Moreover, the use of simulations and the physics-based digital twin approach expedites the packaging design process, enabling the testing of different packaging materials, or testing different vent positions, shapes, and sizes. This saves time and resources, as the number of potential packaging designs that must be tested experimentally can be reduced.

It is noteworthy to mention here that in the predicted values from the simulations, the effects from secondary packaging and the effect of stacking are not included. In principle, it is possible to simulate several packages stacked together inside a secondary package, however, this is computationally expensive. Additionally, we assumed constant thermophysical properties for the fruit in the simulation, including size, thermal conductivity, and fruit density, among others. However, in reality, all fruit possess an inherent biological variability due to preharvest conditions. Using a Monte Carlo approach, such variability can be accounted for to create a virtual population of fruit with different thermophysical properties (Onwude et al., 2022).

One key complementary insight that these simulations provided is the quantification and spatial distribution of the risk of condensation. As condensation can simultaneously occur even on locally different parts of the same fruit, point measurements for dew point are often inadequate to quantify condensation. Moreover, several studies have reported the challenges in measuring condensation experimentally (Linke et al., 2021). Direct gravimetric methods to measure the weight of the condensate require a very high-precision weighing scale. Indirect measurements, such as electric signal sensors to measure wetness, also provide only point measurements (Linke et al., 2021). Here, simulations have a key added value. For instance, critical regions vulnerable to condensation can be identified within the packaging spatio-temporally. As physics-based digital twins use actual sensor data as input, the predictions for the risk of condensation are more representative as they consider the effect of fluctuations in air temperature and humidity in the package headspace.

4.3. Outlook

To improve future packaging studies, we propose an approach that combines climatic chamber experiments with simulations by digital twins of packed fruits. In the present study, constant airspeed, temperature and humidity were maintained around the fruit in the laboratory

experiments in the climatic chamber. However, the use of climatic chambers that offer the possibility of feeding variable or fluctuating input profiles for airspeed, temperature and/or relative humidity would provide several advantages. First, this would enable the reproduction of specific cold chains with unique hygrothermal conditions by using real monitoring sensor data. Second, this will serve as the option to study the impact of temperature fluctuations on condensation inside the packaging. Finally, the smaller chamber size will allow for better observation of condensation, for instance, by installing sensors or automated visual observations with cameras. Nevertheless, the availability of such chambers can be limited by high installation and maintenance costs. Furthermore, some parameters, including air speed, cannot always be controlled sufficiently.

Digital twins of packed fruits deploying physics-based models help alleviate the constraints of lab experiments. By this, testing of a multitude of input (i.e., packaging types, dimensions, materials, etc.) and output variables (different models for transpiration, respiration, condensation, etc.) is possible. Especially, condensation or microbial growth models serve a clear benefit compared to laboratory tests, where it can be challenging to control for various parameters. Furthermore, these output parameters are available in a spatio-temporal manner, making it possible to quantify hygrothermal heterogeneities inside different packages. Such synergistic approaches for packaging design are essential, as simulations and physics-based models often rely on experimental calibration. Simulations are therefore appropriate when a relative comparison is required. For instance, in this study, we compared the influence of different packages. However, experimental studies are indispensable when the absolute values of fruit quality metrics need to be evaluated, such as TSS or firmness. In this sense, experiments and simulations provide complementary information.

5. Conclusions

In the present study, we presented the pros and cons of laboratory experiments and simulations in the context of designing packaging for berries. We highlighted how both these approaches could be combined synergistically to obtain complementary information on strawberry packaging for longer shelf life. Our results revealed that the temperatures of the fruit inside the package do not differ significantly between the tested packaging designs (A) top sealed paperboard, (B) closed and (C) open plastic clamshell. This finding was in line with the similar measured temperature-dependent fruit quality parameters (i.e., TSS, acidity, and color) for the three packages. When testing real strawberry fruits with different harvest dates or cultivation types, the preharvest variability between different batches can significantly influence fruit quality in terms of maximal storage and shelf life. Moreover, preharvest weather conditions, such as excessive rainfall during fruit growth, has a considerable influence on the amount of decayed fruit. By simulation analyses, we found that package C has an increased heterogeneity of quantified parameters inside the packaging compared to A and B. Overall, the packaging performance of packaging A was determined as the best in terms of quality, mass loss and condensation. This is primarily due to the presence of vents in the flow direction. Therefore, ventilation holes in the package have a more significant influence on the air flow inside the package than the packaging materials.

CRediT authorship contribution statement

T.D. and S.S. conceptualized the study and acquired funding; T.D. did the project administration; C.S., S.S. and S.G. performed the investigation, developed the methodology; L.K. executed the laboratory experiments with key input from S.G.; C.S. performed the simulation experiments; C.S., S.S. and S.G. did the data analysis; C.S. and S.S. did the visualization; C.S. and S.S. wrote the original draft of the paper; S.G., D.O., K.S., and T.D. performed critical review and editing.

Declaration of Competing Interest

The authors declare that they have no known competing financial interests or personal relationships that could have appeared to influence the work reported in this paper.

Data Availability

Data will be made available on request.

Acknowledgments

The authors would like to thank André Ançay and Nathan Laruelle for their support of the storage experiments. The authors declare that this study received funding from the Coop Sustainability Fund and the Swiss National Science Foundation SNSF (project 200021_169372). The funder was not involved in the analysis, interpretation of data, writing this article, or the decision to submit it for publication. This manuscript has been released as a preprint on engrXiv.

References

Al-Asmar, A., Giosafatto, C. V. L., Sabbah, M., Sanchez, A., Santana, R. V., & Mariniello, L. (2020). Effect of mesoporous silica nanoparticles on the physicochemical properties of pectin packaging material for strawberry wrapping. *Nanomaterials, 10*(1), 52. https://doi.org/10.3390/nano10010052

ASHRAE. (2010). *Thermal properties of foods. In 2010 ASHRAE handbook: refrigeration* (pp. 19.1–19.31). Atlanta: ASHRAE (SI Edition).

Becker, B. R., Misra, A., & Fricke, B. A. (1996). Bulk refrigeration of fruits and vegetables part I: Theoretical considerations of heat and mass transfer. *HVAC and R Research, 2*(2), 122–134. https://doi.org/10.1080/10789669.1996.10391338

Bovi, G. G., Caleb, O. J., Ilte, K., Rauh, C., & Mahajan, P. V. (2018). Impact of modified atmosphere and humidity packaging on the quality, off-odour development and volatiles of 'Elsanta' strawberries. *Food Packaging and Shelf Life, 16*, 204–210. https://doi.org/10.1016/J.FPSL.2018.04.002

Bovi, G. G., Caleb, O. J., Klaus, E., Tintchev, F., Rauh, C., & Mahajan, P. V. (2018). Moisture absorption kinetics of FruitPad for packaging of fresh strawberry. *Journal of Food Engineering, 223*, 248–254. https://doi.org/10.1016/j.jfoodeng.2017.10.012

Bovi, G. G., Caleb, O. J., Rauh, C., & Mahajan, P. V. (2019). Condensation regulation of packaged strawberries under fluctuating storage temperature. *Packaging Technology and Science, 32*(11), 545–554. https://doi.org/10.1002/pts.2470

Feliziani, E., & Romanazzi, G. (2016). Postharvest decay of strawberry fruit: Etiology, epidemiology, and disease management. *Journal of Berry Research, 6*(1), 47–63. https://doi.org/10.3233/JBR-150113

Ferrua, M. J., & Singh, R. P. (2011). Improved airflow method and packaging system for forced-air cooling of strawberries. *International Journal of Refrigeration, 34*(4), 1162–1173. https://doi.org/10.1016/j.ijrefrig.2011.01.018

Getahun, S., Ambaw, A., Delele, M., Meyer, C. J., & Opara, U. L. (2017). Analysis of airflow and heat transfer inside fruit packed refrigerated shipping container: Part II – Evaluation of apple packaging design and vertical flow resistance. *Journal of Food Engineering, 203*, 83–94. https://doi.org/10.1016/j.jfoodeng.2017.02.011

Han, J. W., Qian, J. P., Zhao, C. J., Yang, X. T., & Fan, B. L. (2017). Mathematical modelling of cooling efficiency of ventilated packaging: Integral performance evaluation. *International Journal of Heat and Mass Transfer, 111*, 386–397. https://doi.org/10.1016/j.ijheatmasstransfer.2017.04.015

Hancock, J. F. (2020). *Strawberries* (Vol. 34). CABI.

Hikawa-Endo, M. (2020). Improvement in the shelf-life of japanese strawberry fruits by breeding and post-harvest techniques. *The Horticulture Journal, 89*(2), 115–123. https://doi.org/10.2503/HORTJ.UTD-R008

Jalali, A., Rux, G., Linke, M., Geyer, M., Pant, A., Saengerlaub, S., & Mahajan, P. (2019). Application of humidity absorbing trays to fresh produce packaging: Mathematical modeling and experimental validation. *Journal of Food Engineering, 244*, 115–125. https://doi.org/10.1016/J.JFOODENG.2018.09.006

Jarvis, W.R. (1977). Botryotinia and Botrytis species: taxonomy, physiology and pathogenicity - A guide to the literature. Agriculture Canada.

Junior, O. J. C., Youssef, K., Koyama, R., Ahmed, S., Dominguez, A. R., Mühlbeier, D. T., & Roberto, S. R. (2019a). Control of gray mold on clamshell-packaged 'benitaka' table grapes using sulphur dioxide pads and perforated liners. *Pathogens 2019, 8*(4), 271. https://doi.org/10.3390/PATHOGENS8040271

Junior, O. J. C., Youssef, K., Koyama, R., Ahmed, S., Dominguez, A. R., Mühlbeier, D. T., & Roberto, S. R. (2019b). Control of gray mold on clamshell-packaged 'benitaka' table grapes using sulphur dioxide pads and perforated liners. *Pathogens 2019, 8*(4), 271. https://doi.org/10.3390/PATHOGENS8040271

Kelly, K., Madden, R., Emond, J. P., & do Nascimento Nunes, M. C. (2019). A novel approach to determine the impact level of each step along the supply chain on strawberry quality. *Postharvest Biology and Technology, 147*, 78–88. https://doi.org/10.1016/J.POSTHARVBIO.2018.09.012

Lahlali, R., Serrhini, M. N., Friel, D., & Jijakli, M. H. (2007). Predictive modelling of temperature and water activity (solutes) on the in vitro radial growth of Botrytis

cinerea Pers. *International Journal of Food Microbiology, 114*(1), 1–9. https://doi.org/10.1016/j.ijfoodmicro.2006.11.004

Lai, Y.-P., Emond, J.-P., & Nunes, M. C. N. (2011). Environmental conditions encountered during distribution from the field to the store affect the quality of strawberry ('Albion'). *Proc Florida State Hortique Soc* (Vol. 124).

Li, C., Tang, H., Wang, J., Zhong, Z., Li, J., & Wang, H. (2021). Field study to characterize customer flow and ventilation rates in retail buildings in Shenzhen, China. *Building and Environment, 197*, Article 107837. https://doi.org/10.1016/J.BUILDENV.2021.107837

Linke, M., & Geyer, M. (2013). Condensation dynamics in plastic film packaging of fruit and vegetables. *Journal of Food Engineering, 116*(1), 144–154. https://doi.org/10.1016/j.jfoodeng.2012.11.026

Linke, M., Praeger, U., Mahajan, P. V., & Geyer, M. (2021). Water vapour condensation on the surface of bulky fruit: Some basics and a simple measurement method. *Journal of Food Engineering, 307*, Article 110661. https://doi.org/10.1016/J.JFOODENG.2021.110661

Nalbandi, H., & Seiiedlou, S. (2020). Sensitivity analysis of the precooling process of strawberry: Effect of package designing parameters and the moisture loss. *Food Science & Nutrition, 8*(5), 2458–2471.

do Nascimento Nunes, M. C., Nicometo, M., Emond, J. P., Melis, R. B., & Uysal, I. (2014). Improvement in fresh fruit and vegetable logistics quality: berry logistics field studies. *Philosophical Transactions of the Royal Society A: Mathematical, Physical and Engineering Sciences, 372*(2017), Article 20130307. https://doi.org/10.1098/rsta.2013.0307

Onwude, D., Bahrami, F., Shrivastava, C., Berry, T., Cronje, P., North, J., Kirsten, N., Schudel, S., Crenna, E., Shoji, K., & Defraeye, T. (2022). Physics driven digital twins to quantify the impact of pre and postharvest variability on the end quality evolution of orange fruit. *EngrXiv*.

Opara, U. L., & Zou, Q. (2007). Sensitivity analysis of a CFD modelling system for airflow and heat transfer of fresh food packaging: Inlet air flow velocity and inside-package configurations. *International Journal of Food Engineering, 3*(5), 1–13. https://doi.org/10.2202/1556-3758.1263

OriginLab. (2022). Origin® 2022.

Pathare, P. B., Opara, U. L., Vigneault, C., Delele, M. A., & Al-Said, F. A. J. (2012). Design of packaging vents for cooling fresh horticultural produce. *In Food and Bioprocess Technology* (Vol. 5,(Issue 6), 2031–2045. https://doi.org/10.1007/s11947-012-0883-9

Peano, C., Giuggioli, N. R., & Girgenti, V. (2014). Effect of different packaging materials on postharvest quality of cv. Envie2 strawberry. *International Food Research Journal, 21*(3), 1165–1170.

R Core Team. (2020). R: A Language and Environment for Statistical Computing.

Shin, Y., Liu, R. H., Nock, J. F., Holliday, D., & Watkins, C. B. (2007). Temperature and relative humidity effects on quality, total ascorbic acid, phenolics and flavonoid concentrations, and antioxidant activity of strawberry. *Postharvest Biology and Technology, 45*(3), 349–357. https://doi.org/10.1016/J.POSTHARVBIO.2007.03.007

Shoji, K., Schudel, S., Onwude, D., Shrivastava, C., & Defraeye, T. (2022). Mapping the postharvest life of imported fruits from packhouse to retail stores using physics-based digital twins. *Resources, Conservation and Recycling, 176*, Article 105914. https://doi.org/10.1016/J.RESCONREC.2021.105914

Shrivastava, C., Schudel, S., Shoji, S., Onwude, D., Pereira da Silva, F., Turan, D., … Defraeye, T. (2022). Digital twins for selecting the optimal ventilated strawberry packaging based on the unique hygrothermal conditions of a shipment from farm to retailer. *engrXiv*. https://doi.org/10.31224/2553

Snow, D. (1949). The germination of mould spores at controlled humidities. *Annals of Applied Biology, 36*(1), 1–13. https://doi.org/10.1111/j.1744-7348.1949.tb06395.x

Sousa-Gallagher, M. J., Mahajan, P. V., & Mezdad, T. (2013). Engineering packaging design accounting for transpiration rate: Model development and validation with strawberries. *Journal of Food Engineering, 119*(2), 370–376. https://doi.org/10.1016/j.jfoodeng.2013.05.041

Tano, K., Kamenan, A., & Arul, J. (2009). Respiration and transpiration characteristics of selected fresh fruits and vegetables. *Agronomie Africaine, 17*(2), 103–115. https://doi.org/10.4314/aga.v17i2.1662

Thompson, J. F., Mitchell, F. G., & Rumsay, T. R. (2008). *Commercial cooling of fruits, vegetables, and flowers (p. 61)*. University of California, Agriculture and Natural Resources,.

Tijskens, L. M. M., & Polderdijk, J. J. (1996). A generic model for keeping quality of vegetable produce during storage and distribution. *Agricultural Systems, 51*(4), 431–452. https://doi.org/10.1016/0308-521X(95)00058-D

van Boekel, M. A. J. S. (2008). Kinetic Modeling of Food Quality: A Critical Review. *Comprehensive Reviews in Food Science and Food Safety, 7*(1), 144–158. https://doi.org/10.1111/J.1541-4337.2007.00036.X

Williamson, B., Duncan, G. H., Harrison, J. G., Harding, L. A., Elad, Y., & Zimand, G. (1995). Effect of humidity on infection of rose petals by dry-inoculated conidia of Botrytis cinerea. *Mycological Research, 99*(11), 1303–1310. https://doi.org/10.1016/S0953-7562(09)81212-4

Williamson, B., Tudzynski, B., Tudzynski, P., & Van Kan, J. A. L. (2007). Botrytis cinerea: the cause of grey mould disease. *Molecular Plant Pathology, 8*(5), 561–580. https://doi.org/10.1111/J.1364-3703.2007.00417.X

Wu, W., Cronje, P., Verboven, P., & Defraeye, T. (2019). Unveiling how ventilated packaging design and cold chain scenarios affect the cooling kinetics and fruit quality for each single citrus fruit in an entire pallet. *Food Packaging and Shelf Life, 21*, Article 100369.

Zhao, X., Xia, M., Wei, X., Xu, C., Luo, Z., & Mao, L. (2019). Consolidated cold and modified atmosphere package system for fresh strawberry supply chains. *LWT, 109*, 207–215. https://doi.org/10.1016/j.lwt.2019.04.032